

Correlation between size and distribution of pre- and post-proof test level flaw of draw-abraded fiber

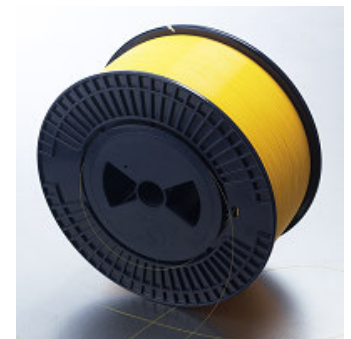
Author

S. Bhaumik

Document: WP0010

Abstract

The mechanical reliability of single mode optical fiber is determined by the presence of surface flaws such as particles from the atmosphere during drawing or abrasion damage of the fiber surface by physical contact with any hard surface or drawing equipment and its size distribution, which are produced by normal fiber production methods. Proof testing is a common technique to ensure minimum strength of the fiber and eliminate the flaws whose sizes are dependent on the stress applied during proof testing. This paper describes the relation between the size and distribution of pre-and post-proof test flaws.



Keywords

Optical Fiber; Strength; flaw distribution

Optical waveguide used in telecommunication is proof tested at 1% strain, which is equivalent to 700 Mpa stress and corresponds to a surface flaw size of approximately 0.85 μm . Thus proof testing with 1% strain eliminates surface flaws above 0.85 μm . The proof-test level flaws are rarely found in high quality optical fiber. A wide distribution of flaws can be intentionally created by abrasion¹ and fusion of refractory particles² on to the uncoated fiber surface and drawing with a dirty atmosphere.³ To evaluate the importance of these flaws and its relation with the flaws present after proof testing for long term reliability prediction, these kinds of intentionally created flaws are employed.

Break source analysis (BSA) is generally used to determine the cause of failure in optical fiber. In addition, magnitude and mode of stress at failure can be calculated from mirror radius and flaw size.^{4,5,6} Previous studies showed that fiber strength distribution can be represented statistically by applying dynamic and static tensile load and scaled for failure probability prediction for a range of fiber lengths.^{1,3,7} A significant time dependence of strength under static test was found in weak spots on optical fiber caused by physical contact with glass during drawing.³

This paper highlights the results of a series of tests conducted with various draw abraded optical fiber to describe the relation between the size and distribution of pre- and post-proof test flaws in terms of corresponding fracture stress.

Fiber strength

Silica glasses used in optical fiber applications behave as elastic bodies up to its breaking strength. The elastic strains are produced by elongations and rotations of the bonds between the atoms comprising the glass. Gradual increase in elastic modulus with increasing strain has been observed for fused silica and typical nonlinear extension curve has been reported as

$$E/E_0 = 1 + \alpha\epsilon \quad \text{————— Eq. (1)}$$

where E (typical value is 71.9 Gpa) and E_0 are the tensile moduli at a strain ϵ and at zero strain, respectively. The parameter α is given by 5.75 for fused silica.⁸ Optical fibers are coated to protect the glass surface. The fraction of tensile load carried by a uniformly thick, linear elastic coating is given by

$$E_c A_c / (E_c A_c + E_g A_g) \quad \text{————— Eq. (2)}$$

Where E is the elastic modulus, A is the cross-sectional area, and subscripts g and c represent glass and coating respectively. The theoretical strength of glass fibers is estimated to 20 Gpa and several investigators found values of approximately 6 and 14 Gpa at room temperature and liquid nitrogen temperature, respectively.^{9,10} But in homogeneities and flaws reduce fracture strength, which can be represented by the well known fracture mechanics equation

$$\sigma_c = K_{Ic} / Y(a_c)^{1/2} \quad \text{————— Eq. (3)}$$

Where σ_f = fracture strength, K_{Ic} = fracture toughness or critical stress intensity factor (for silica glass $0.74 \text{ MPa}\sqrt{\text{m}}$), Y = flaw geometry factor (for half-elliptical surface crack $Y = 1.25$, for circular crack $Y = 1.117$,^{5,13}) and a_c = critical flaw size.

Eq. (3) can be used to calculate fracture strength of silica glass fiber containing a known flaw size. Similarly, flaw size can be calculated from known fracture strength. The fracture strength of an optical fiber sample represents strength corresponding to the largest flaw or weakest site and typical failure strength decreases as sample length increases. As flaws on the glass fiber are independent and randomly distributed and statistical in nature, the Weibull probability plot is generally used to represent flaw distribution.

Proof testing is a conventional method of assuring the minimum strength level. It has been reported that strength level of proof tested fiber is influenced by the unloading rate in the proof testing cycle.^{12,13} This is because of crack growth occurring during the unloading cycle due to stress corrosion. Assuming that unloading is rapid enough to suppress the flaw growth, the fiber fracture condition in the proof test is determined by using Eq. (3). The minimum strength, σ_m of proof tested fiber is given as

$$\sigma_m = \{B(n+1) \sigma_p \sigma_p^{n-2}\}^{1/(n+1)} \text{ ————— Eq. (4)}$$

where σ_p is the loading rate, B is a constant and n is the crack growth parameter.¹⁴

Fracture behavior in brittle materials such as glass has been studied and the application of break source analysis (BSA) to determine the mode of failure is reported. During the fracture process, the crack grows from its original size until it approaches critical velocity. This behavior includes a flat origin known as mirror, a slightly roughened region called mist and a region of radiating ridges and valleys called hackle, and a boundary at which large-scale crack branching occurs. This behavior is illustrated in Fig. 1 and well documented in literature.^{15,16,17}

It has been reported that the distance from the fracture origin to the mirror-mist boundary (which is known as mirror radius) is proportional to the flaw size which can be used to calculate fracture stress by using Eq. (3). The flaw size is generally $1/10^{\text{th}}$ of mirror radius.¹⁸ Thus, flaw size and actual stress at failure can be calculated by measuring the size of the mirror. Fracture stress can be directly calculated from mirror radius by the following equation:

$$\sigma_f = 1.72 / \sqrt{a_c} R \text{ Mpa ————— Eq. (5)}$$

where, R is mirror radius in meter as found in previous studies.⁶ Some other studies reported that the ratio of the mirror radius to the critical flaw size is constant but the ratio of the mirror radius to the initial flaw size is not a constant and varies with time under load.¹⁹ If time under load during proof testing (commonly known as dwell time) is constant, Eq. (3) can be used to calculate fracture stress by taking critical flaw size equal to $1/10^{\text{th}}$ of mirror radius.

The local environment at the surface flaw of silica fiber can have substantial effect on the strength and time-dependent fracture. Water in the environment is primarily responsible for the crack growth. Under constant applied stress below the inert strength of fiber, fracture can occur after a period of time in a humid environment. This behavior and mechanism are known as static fatigue and stress corrosion respectively.

Experimental

Single mode silica optical fiber of diameter $125 \mu\text{m}$ were drawn and coated with standard acrylate polymer coating. In order to obtain a wide range of flaw distribution near proof-testing level, fibers were drawn in a dirty manufacturing environment and abraded during drawing in a

controlled manner. About 400 km of draw-abraded fibers were drawn with four different extent of abrasion (100 km each and represented as Abr 1 to 4) and proof tested with 1.0% strain. The proof testing break ends were carefully collected and mirror radius measurements were performed using optical and electron microscope. Fracture stress was calculated by using Eq (3) and taking flaw size as $1/10^{\text{th}}$ of mirror radius.

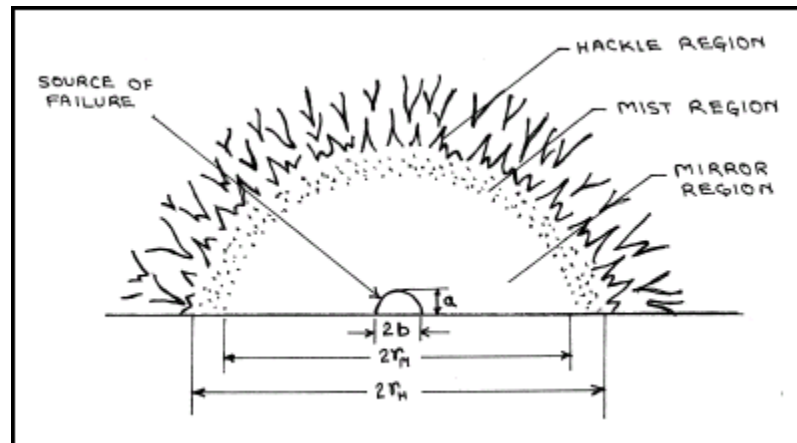


Fig. 1. Schematic diagram showing fracture surface. The variables a and b are the radii of idealized semi-elliptical flaw, r_m is the mirror radius and r_H is the hackle radius.

The following tests were performed with the proof-tested pieces of the same draw-abraded fiber to measure size and distribution of post proof test flaws:

- **Dynamic Tensile Strength Test**— This test was conducted as per FOTP- 28C (EIA/TIA) with a 0.5 m sample length and 25 mm/min extension rate at $25(\pm 2)^{\circ}\text{C}$ temperature and $50 (\pm 5)\%$ relative humidity. Hundred readings per category of draw-abraded fiber had been taken.
- **Static Tensile Strength Test**—Time to failures were measured by applying 4.3 GPa static tensile stress on fiber 2 m in length. All tests were conducted at $25(\pm 2)^{\circ}\text{C}$ temperature and $50 (\pm 5)\%$ relative humidity. Thirty readings per category of draw-abraded fiber had been taken. Static tensile stress was kept close to fracture stress of the fibers in order to get more failure at shorter times.

Results and discussion

The proof-test level flaw size and its distribution of draw-abraded fibers in terms of corresponding fracture stress have been calculated by using Eq. (3). The Weibull plot of this distribution is shown in Fig. 2.

| | Break Source Analysis (BSA) | | | | Dynamic Tensile Load | | Static Tensile Load | |
|----------|-----------------------------|---------------------|------------------------------|----------|------------------------------|----------|------------------------------|----------|
| | Breaks/100 km | No. of break tested | Median Fracture Stress (Mpa) | M- value | Median Fracture Stress (Gpa) | M- value | Median Time to failure (sec) | M- value |
| Abr.# 01 | 25 | 19 | 565 | 5.4 | 4.332 | 22 | 54 | 1.3 |
| Abr.# 02 | 28 | 22 | 445 | 4.9 | 4.325 | 15 | 60.5 | 1.3 |
| Abr.# 03 | 31 | 28 | 635 | 20.2 | 4.475 | 34 | 92 | 11 |
| Abr.# 04 | 44 | 38 | 559 | 5.4 | 4.379 | 20 | 67 | 2 |

Table 1. Experimental results of various abraded fibers.

| | BSA | | Dynamic Tensile Load | | Static Tensile Load | |
|----------|------------------------------|------|------------------------------|------|------------------------------|------|
| | Median Fracture Stress (Mpa) | M | Median Fracture Stress (Gpa) | M | Median Time to failure (sec) | M |
| Abr.# 01 | 1.27 | 1.10 | 1.00 | 1.47 | 1.00 | 1.00 |
| Abr.# 02 | 1.00 | 1.00 | 1.00 | 1.00 | 1.12 | 1.00 |
| Abr.# 03 | 1.43 | 4.12 | 1.03 | 2.27 | 1.70 | 8.46 |
| Abr.# 04 | 1.26 | 1.10 | 1.01 | 1.33 | 1.24 | 1.54 |

Table 2. Normalized values of the Weibull parameters of various abraded fibers.

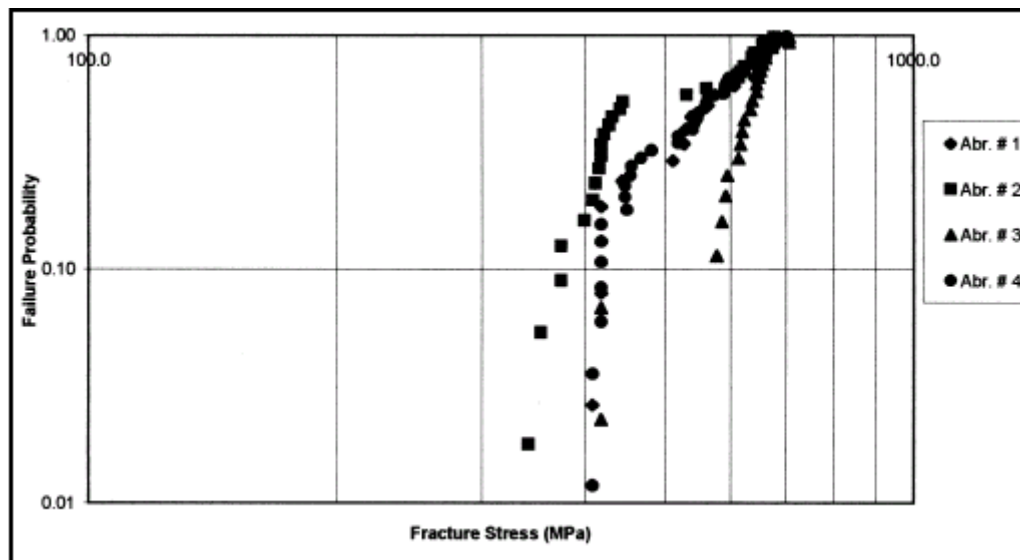


Fig. 2. Weibull probability distribution of fracture stress corresponding to proof test level flaws of various draw-abraded fibers.

The details of abraded fibers, i.e., breaks per 100 km, number of break tested and Weibull parameters, are given in Table 1 under BSA. The highest number of proof testing breaks were found in abraded fiber No. 4. Pre proof test level flaw sizes of abraded fiber No. 3 were significantly lower than the other draw-abraded fibers. Multi-modal behavior was very prominent in abraded fiber No. 1, 2 and 4, resulting low M-value. Flaws were found more scattered above 20% probability level in all cases.

The post-proof testing flaw or strength distribution of draw-abraded fibers measured by dynamic and static tensile load have been shown in Figs. 3 and 4 respectively and Weibull parameters are listed in Table 1. Here also abraded fiber No. 3 showed the highest median

fracture stress and time to failure among all abraded fibers as shown by BSA. A similar kind of multi-modality as described in previous paragraph, i.e., more scattering in higher strength region, exists in both pre- and post-proof test level flaw distribution. In spite of existence of multi-modality, dynamic tensile strength test results showed less scattered

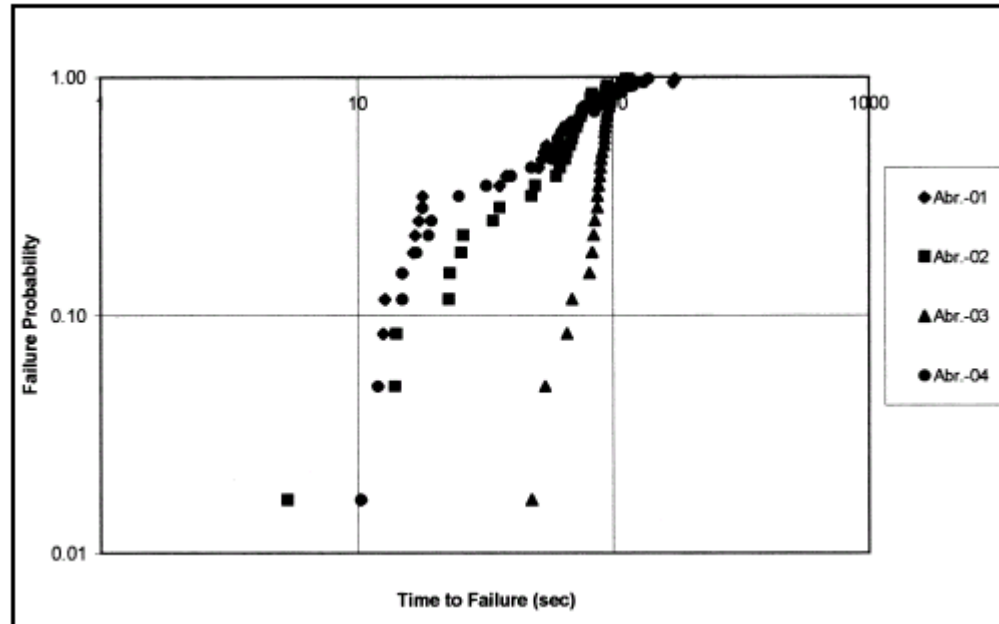


Fig. 3. Weibull probability distribution of time-to-failure under static tensile load of various post-proof tested draw-abraded fibers.

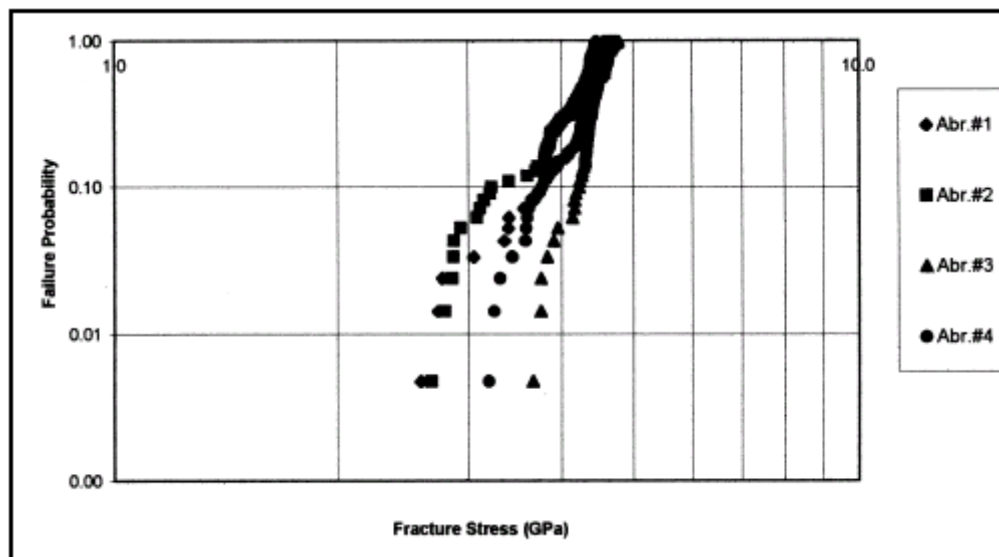


Fig. 4. Weibull probability distribution of fracture stress under dynamic tensile load of various post-proof tested draw-abraded fibers.

strength distribution resulting in higher M- values. Weibull parameters of various abraded fibers are compared and shown in Table 2. The normalized values in Table 2 specify that the dynamic tensile strength of the fibers are close to each other and less affected by extent of draw abrasion compared to static tensile

test, whereas static tensile test results were comparatively more affected by extent of draw abrasion because of longer sample length. This observation signifies that the intrinsic strength distribution of optical fiber measured by dynamic loading with 0.5 m sample is less affected by draw abrasion. However, the extrinsic flaws, which are important for long term reliability of optical fiber, are affected by draw abrasion.

Conclusion

- Flaws produced by particle and draw abrasion are conveniently used for correlating size and distribution of pre- and post-proof test level flaws.
- Flaws produced by draw-abrasion control strength distribution of both pre- and post-proof test fibers.
- Size and distribution of flaws both for microscopic (i.e., proof test level) and submicroscopic (i.e., post-proof test level) level depend on the extent of particle and draw abrasion.
- Draw abrasion has shown comparatively less effect on intrinsic strength of the fiber.
- According to the relationship observed between pre- and post-proof test level flaws, it can be concluded that the post-proof test level flaws can be controlled by controlling the proof test level flaw sizes and its distribution.

References

1. G.S. Glaesemann, "The mechanical behavior of large flaws in optical fiber and their role in reliability predictions," *IWCS Conference Proceedings*, 1992, pp. 698-704.
2. T. Breuls and T. Svensson, "Strength and fatigue of zirconia induced weak spots in optical fibers," *SPIE*, 2074, 1994, p. 78.
3. A. Breuls and T. Svensson, "Strength and fatigue of different kind of weak spots from the manufacture of optical glass fibers," *SPIE*, 2290, pp. 211-220.
4. S.W. Freiman, "Brittle Fracture Behaviour of Ceramics," *Ceramic Bulletin*, 67 (2), 1988, pp. 392-402.
5. V.D. Frechette, "Failure Analysis of Brittle Materials," in the *Advances in Ceramics Series*, Vol. 28, 1990.
6. Linda K. Baker and G.S. Glaesemann, "Break source analysis: Alternate mirror measurement method," *IWCS Conference Proceedings*, 1998, pp. 933- 937.
7. J. Bjorkman and T. Svensson, "Quick-access to fracture statistics at ultra-wide-range tensile test of optical fibers," *IWCS Conference Proceedings*, 1990, pp. 373-378.
8. F.P. Mallinder and B.A. Proctor, "Elastic constants of fused silica as a function of large tensile strain," *Physics and Chemistry of Glasses* 5, 1964, p. 91.
9. W.B. Hillig, "Sources of weakness and the ultimate strength of brittle amorphous solids," *Modern Aspects of the Vitreous State* (J.D. MacKenzie, ed.), Vol. 2, Butterworth 1962, p. 152.
10. B.A. Proctor, I. Whitney and J.W. Johnson J, "The strength of fused silica," *Proc. R. Soc. London Ser.,A* 297, p. 534.
11. D. Inniss, Q. Zhong and C.R. Kurkjian, "Chemically corroded pristine silica fibers: blunt and sharp flaws?," *J. Am. Ceram. Soc.* 76, 1993, pp. 3173- 3177.
12. T.A. Hanson, ed. "Proof Testing Optical Fibers by Tension," *FOTP-31, EIA/TIA-455-31*, February 1995.
13. "Power-Law Theory of Optical Fiber Reliability," *IEC SC 86A/WG 1*, September 1996.

14. S. Sakaguchi, "Drawing of high strength long-length optical fibers for submarine cables," *IEEE J. of selected areas in communications*, Vol. SAC-2, No 6, November 1984.
15. S.W. Freiman, "Brittle Fracture Behavior of Ceramics," *Ceram. Bulletin*, 67, 2, 1988, pp. 392-402.
16. V.D. Frechette "Failure Analysis of Brittle Materials," *Advances in Ceramic Series*, Vol 28, 1990.
17. H.P. Kirchner and J.W. Kirchner, "Fracture Mechanics of Fracture Mirrors," *J. Am. Ceramic Soc.*, Vol. 62, No. 3-4, 1979, pp. 198-202.
18. Li Tingye, "Optical Fiber Communications," p. 235-238.
19. J.J. Mecholsky, S.W. Gonzales and S.W. Freiman, *J. Am. Ceramic Soc.*, 63, 1980, pp. 577-580.

Optical Fiber

Whitepaper



Sterlite Technologies Limited

**Aurangabad
Bangkok
Beijing
Boston
Haridwar
Johannesburg
Dadra
London
Moscow
Mumbai
New Delhi
Piparia
Pune
Rakholi
Shanghai**

**Phone: +91-20-30514000
communications@sterlite.com**

www.sterlitetechnologies.com